International Journal of Scientific Research and Engineering Development-–Volume 8 Issue 4, July-Aug 2025
Available at www.ijsred.com

RESEARCH ARTICLE OPEN ACCESS

Evaluation of Fault Compartmentalization and Seal Integrity of an Onshore Field in the Niger Delta Basin, Nigeria

[1]Enyiazu, H.C. and [2]Ugwueze, C.U.
[1]Centre for Petroleum Geosciences, University of Port Harcourt, greathenryben@yahoo.com, +2348060797206,
[2]Department of Geology, University of Port Harcourt, charles.ugwueze@uniport.edu.ng, +2348035632241, ORCID: https://orcid.org/0000-0002-0904-1621

Abstract:

A static model approach was used to investigate the sealing property and trend of the XAS reservoir within the Onshore Niger Delta Basin, utilizing a method that was aimed at identifying sealing faults that might have compartmentalized oil and gas accumulations. Field correlation was established, which facilitated the prediction of facies variation within the reservoir and allowed for constructing a more representative static model. The model proposed five resolvable genetic units to be interpreted. Two main reservoir flow units were also identified from the model. Structural compartmentalization was assessed by measuring the shale-gouge ratio (SGR), fault permeability, and fault zone thickness of the sand-on-sand juxtapositions of the relevant intra-reservoir faults. The in-place volume of oil calculated was 1312×10^6 STB, and the GIIP was determined to be 805×10^6 Bscf. The fault juxtaposition analysis recognized areas of interest where faults were juxtaposed above the oil-water contact (OWC). The SGR, fault thickness, and permeability of the fault within the juxtaposed zones indicated that while the faults are not likely to have compartmentalized the reservoir into distinct pressure compartments, they had the potential to operate as fluid flow baffles across the faults.

Keywords: **Fault Compartmentalization, Seal Integrity, Shale-Gouge Ratio, Juxtapositions, Onshore Niger Delta Basin**

I. INTRODUCTION

Faults are a central element in the formation of hydrocarbon traps and exert a significant influence on the viability of fault-controlled exploration prospects. Evaluating faults' sealing capacity is crucial for reducing the risks associated with exploration and production, particularly in faulted reservoirs. In cases where faults crosscut reservoir sequences, it is important to examine the possibility of sealing in different segments of the fault system. The examination helps recognize whether a fault will trap hydrocarbons or allow their migration (Watts, 1987).

Reservoir compartmentalisation is the segregation of hydrocarbon accumulations into individual fluid or pressure compartments; it has also been defined as the existence of petroleum accumulations in discrete individual compartments in the reservoir (Jolley *et al*., 2007a & b). The basic seal types that can sustain compartmentalization are static and dynamic seals. Sealing faults play a major role in the traps of many hydrocarbon reservoirs; they can turn a relatively large and continuous hydrocarbon reservoir into

compartments which become collections of smaller reservoirs. Each compartment may have its own pressure and fluid characteristics, which, in turn, may affect efficient and effective field development and subsequent hydrocarbon recovery. When faults do not form seals, they can hinder the accumulation of hydrocarbons because they ultimately become migration pathways. There are several geological mechanisms by which faults can serve as effective seals:

a. Smearing of clay: Smearing of ductile clay layers along the fault plane at the time of faulting can result in the formation of a continuous impermeable barrier of high capillary entry pressure. The smeared clay would generally cease hydrocarbon migration by physically separating permeable layers (Yielding *et al*., 1997).

b. Juxtaposition Sealing: Permeable reservoir rocks are, in this instance, juxtaposed against impermeable strata, usually shale, at elevated entry pressures. The juxtaposition of permeability and porosity contrast between the layers restricts hydrocarbon flow across the fault (Lindsay *et al.,* 1993).

c. Diagenetic Sealing: Post-faulting reactions such as cementation may alter the permeability of a previously open fault zone. Mineral precipitation may have filled pore spaces within the fault and drastically reduced porosity, creating a seal (Knipe, 1997).

d. Cataclastic Sealing: If mechanical deformation disintegrates the sand grains during faulting, a gouge formed is fine-grained. The crushed-up rock material increases capillary entry pressure, potentially preventing hydrocarbons from flowing through the fault (Fisher & Knipe, 2001).

For fault seal prediction to be effective, sealing mechanisms must be connected with measurable subsurface properties like lithology, fault geometry, and displacement. Practical predictive models tend to work best when they are based on routinely acquired geology and geophysics data, such as well logs and seismic interpretation (Yielding *et al*., 1997). Fault sealing performance depends on both post-faulting and geological conditions. Proper evaluation of these parameters underlies enhanced prediction of hydrocarbon entrapment, reducing fault-bounded reservoir uncertainty (Figure 1).

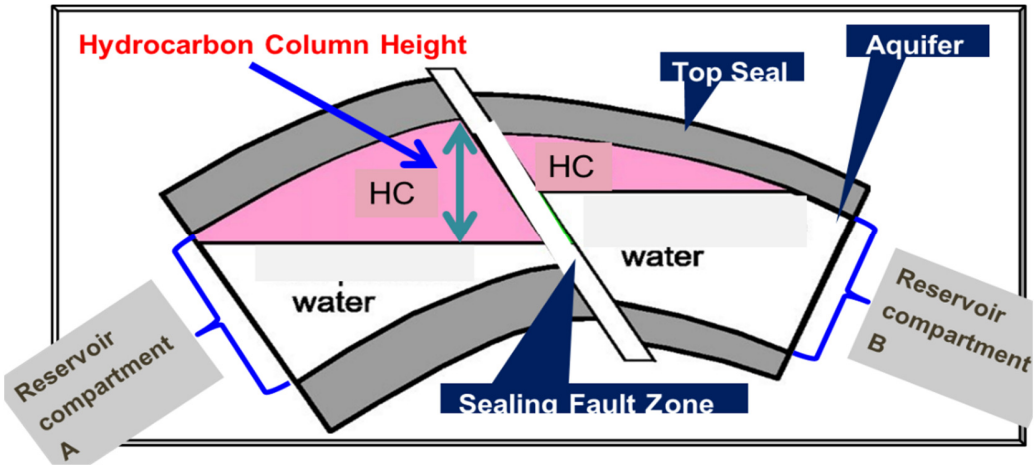

Figure 1: A cartoon diagram showing the sealing fault, compartmentalised reservoir, and hydrocarbon column height (Modified after Bretan *et al*, 2003)

Fault seal analysis is an important procedure in subsurface reservoir management with particular applications in hydrocarbon exploration and CO_2 storage. Juxtaposition, or the contact of various lithological units along a fault plane, is one of the main fault-sealing mechanisms. Sealing is usually efficient where impermeable lithologies, such as shale on shale or other tight units, are juxtaposed. But seal potential is also present where sand bodies of contrasting capillary entry pressures are juxtaposed across a fault. In such cases, there may be an appreciable pressure difference, even in the absence of any sealing fault-zone material, and hydrocarbon column heights may differ by up to 15 meters (Berg, 1975).

One of the most widely applied tools in assessing fault seal capacity is the Shale Gouge Ratio (SGR). It establishes the percent of clay or shale that has entered a fault zone due to faulting and could be applied as an analogue to the probability that a fault would form an effective seal. High SGRs are usually associated with high concentrations of clay and thus a high probability for a fault zone to act as a seal (Yielding *et al*., 1997). The method has proven to be very useful in various studies, including Freeman *et al*. (2010) for the North Sea, in which SGR showed a very good correlation with pressure gradients seen across faults. Another fault seal evaluation model is Clay Smear Potential (CSP), where the quality of the clay smear along faults is assessed. CSP value is proportionate to the continuity of the clay smear as an effective sealer of faults and a fault sealer (Lindsay *et al*., 1993). However, the CSP is also still empirical and of maximum use if interpreted alongside SGR values and general geological interpretations.

The Niger Delta Basin offers useful lessons regarding fault compartmentalisation. Aderoju *et al*. (2019) employed well and seismic data to assess fault seal integrity using both SGR and juxtaposition analysis. The research indicated high SGR values in shale-rich sequences with good seal potential. Likewise, Obaje *et al*. (2021) applied geomechanical analysis and revealed that stress perturbation can cause seal failure, particularly within over-pressured and faulted areas. Adekunle and Aizebeokhai (2020) also confirmed the presence of fault-bounded compartments in Niger Delta turbiditic reservoirs from resistivity and pressure data. Their findings warranted the use of SGR in forming vertical and horizontal seals, particularly in the region's young depobelts.

Despite advancements in fault compartmentalization studies, there are still difficulties in making precise predictions of fault behaviour and fluid flow. Faults are complex and heterogeneous by nature, and therefore difficult to characterize, especially in deep or inaccessible reservoirs. Seismic data resolution and the interpretation of fault geometries tend not to capture small-scale features critical to understanding compartmentalisation. In mature hydrocarbon provinces such as the Niger Delta, where there is a large number of wells and production data, there may be structural attributes in inter-well zones that can either enhance or limit the production of hydrocarbons. Faults, for example, can seal or open fluid flow between reservoir compartments, affecting waterflood efficiency and CO_2 sequestration. Most waterflood projects fail due to unseen subsurface features that alter fluid flow. Forecasting of fault zone properties in the subsurface remains an outstanding challenge with severe implications for fault-fluid interaction on geological and production time scales. The essential solution is to understand how to control geological boundary conditions on fault zone shape.

II. GEOLOGICAL SETTING

The Niger Delta basin, which is one of the biggest regressive deltas in the world, has a peculiar place in geological and economic studies based on its massive sedimentary accumulations and dynamic geological processes (Doust & Omatsola, 1990). The development and evolution of the basin have a close relationship with the tectonic and sedimentary processes that formed the West African continental margin millions of years ago. The basin is in a strategic position where the South Atlantic Ocean began to open in the Cretaceous (Lehner & De Ruiter, 1977). This was when the supercontinent, Gondwana, began to disintegrate. This was a pivotal moment in the regional history that set the stage for the creation of the delta. The fact that the Niger Delta basin is situated at a passive margin, where the continental margin is neither actively involved in the plate tectonic activities nor is being stretched due to cooling-induced subsidence, also played a role in its development.

The basin is a superb model of a sedimentary rift system formed by a combination of extensional tectonics, thermal subsidence, and clastic sediments from the adjacent landmasses. Geologic evolution of the delta focuses on tectonic and sedimentary interaction in the development of basin architecture, which is of great concern in hydrocarbon distribution in such a system. The basin's deposited thick sediments consist of large petroleum reservoirs, and these are dominated by sandstones and shale sequences. Besides, there are also enormous structural traps, such as growth faults and anticlines, which are responsible for the prospectivity for hydrocarbon accumulation.

The Xas Field is situated in Oil Mining Lease (OML) 18, a prominent onshore oil and gas concession in the Onshore Niger Delta. The field itself is located at approximately latitudes 4.30°N and 4.35°N, and longitudes 7.40°E and 7.50°E (Figure 2) in a logistically and environmentally difficult terrain, typical of the wetland system of the Niger Delta (Corredor *et al.*, 2005).

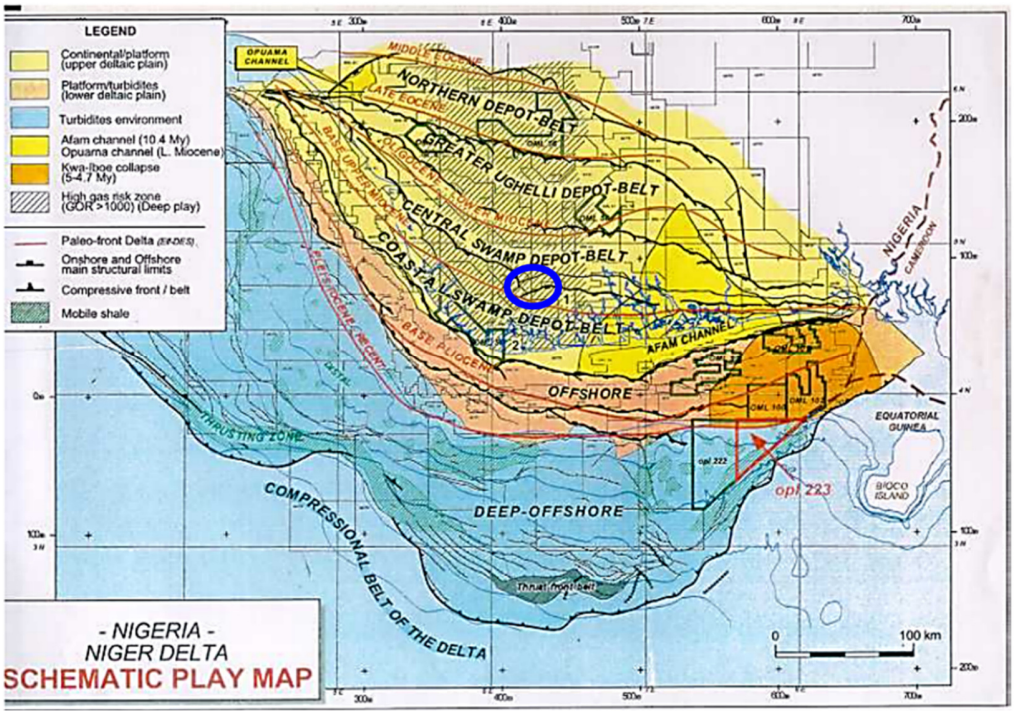

Figure 2: Schematic play map of the Niger Delta, showing the location of the Central and Coastal Swamp Depobelts, and the location of the study area (marked in blue circle) (Corredor *et al*., 2005)

III. MATERIALS AND METHODS

A. Materials

The following data sets were used for the research, including a suite of wireline logs, Oil Water Contact (OWC) and Gas Water Contact (GWC), and two Pre-stack Depth Migrated (PSDM) seismic volumes. The gamma ray (GR) log was used to differentiate between shale and sand formations based on natural radioactivity. This log is particularly useful for identifying reservoir intervals and estimating shale volume. Resistivity logs provided insight into the fluid content of the reservoir rocks by measuring the formation's resistance to electrical current; higher resistivity often indicates the presence of hydrocarbons, whereas lower values may suggest water saturation. The density log was employed to evaluate bulk density, which, when combined with other logs, assists in porosity estimation. It also helps in lithological identification, particularly in distinguishing between shales, sands, and carbonates. Finally, the neutron log was used to estimate hydrogen content in the formation, which correlates with porosity. By comparing neutron and density logs, zones of gas-bearing formations can often be inferred due to the characteristic "crossover" effect observed in such intervals.

The semblance volume was employed primarily to interpret the tops of key reservoir horizons. Meanwhile, the semblance volume was essential in mapping and analyzing fault structures within the seismic cube. The semblance attribute, in particular, proved instrumental for fault identification. It enhanced the visibility of discontinuities within the seismic data, which is vital in geological settings like the Niger Delta basin, where faulting plays a significant role in hydrocarbon entrapment and migration. Where semblance values

were low, they often indicated a fault or another form of structural discontinuity. Thus, this volume served as a key tool in accurately delineating fault planes and understanding their spatial configuration.

When a fault separates two reservoir compartments, comparing the OWC or GWC levels across the fault can reveal whether the fault is sealing. If the contact levels on either side of the fault are at different depths, it suggests that the fault is acting as a barrier, holding back fluids and creating a pressure difference. This is known as a juxtaposition seal or pressure differential evidence of sealing. On the other hand, if the contact levels are the same, it might indicate that the fault is not sealed and fluids are moving freely between compartments.

B. Methods

1) Reservoir Correlation

All the wells penetrating the reservoir were displayed in a unified well section view, allowing for side-by-side comparison of their log profiles. This visualization enabled the identification of repeating log patterns, which served as the basis for selecting key stratigraphic markers, commonly referred to as "well tops." These well tops represented the interpreted boundaries of significant geological units, such as the top and base of the reservoirs.

2) Seismic Interpretation

Seismic interpretation involved horizon picking, fault mapping, and structural framework development. Key reflectors were identified and picked across the 3D seismic cube. These reflectors were generally equivalent to the lithologic contacts or the reservoir tops, i.e., top of an oil/water contact or regional unconformity. The faults were mapped across the seismic volume, and the throws, attitudes, and geometries were measured. Care was taken to focus on faults with high potential to influence fluid communication and compartmentalization within the reflected reservoirs.

3) Structural and Static Model

That structural scheme was subsequently merged with the interpreted faults and seismic horizons to produce a three-dimensional geological model. The horizons were gridded and placed within the scheme of faults to produce a geologically correct model. The fault surfaces were constructed from the interpreted fault sticks; these were used to outline fault blocks. The workflow can include the addition of fault gap corrections, horizon smoothing, among other checks for consistency to produce a correct image of the interpreted geology.

The static model generated was integrated into the geological characteristics within the structural framework, i.e., lithofacies distribution, porosity, permeability, and water saturation. These were generally derived from the well logging, cores, and seismic attributes. The static model was developed using geostatistical modelling, sequential indicator simulation, and kriging. The objective was to construct a realistic image of the heterogeneity of the reservoirs as well as the petrophysical characteristics. Static modelling gave an insight into

the prospective productive zones within the parts of the reservoir and assisted in deciding the sweet spots for drilling. Moreover, it was used as a feed to the dynamic simulation as well as for the volumetric calculations, and hence, it was an intrinsic part of the whole workflow.

4) Fault Analysis

Cross-sections were built for the evaluation of juxtapositions of the reservoir units across faults. Where the sands of the reservoir were juxtaposed across non-reservoir units such as shales, the fault represents a potential seal depending on the capillary entry pressure of the sealing lithology. Fault seal evaluation was conducted by estimating the shale gouge ratio (SGR) or the clay smear potential (CSP) to obtain the quantification of sealing potential depending on the lithological makeup of the fault zone.

5) Facies Description and Modelling Approach

Facies description played a critical role in developing a robust structural and stratigraphic framework for the subsurface reservoir modelling. Facies information derived from well data was utilized to statistically populate the geological model, forming the basis for simulating spatial heterogeneity within the studied field. To simulate the three-dimensional distribution of facies across the reservoir, a geostatistical approach was employed using the Sequential Indicator Simulation (SIS) algorithm. This stochastic modelling technique enabled the generation of multiple equally probable realizations of the reservoir facies architecture, each honouring the observed data at well locations.

Table 1: Facies variogram settings used for modelling the reservoir properties

Facies	Major Direction (m)	Minor Direction (m)
Channel	6079	3000
Upper Shoreface	15989	6079
Lower Shoreface	15989	6079
Heterolith	6079	3000
Shale	assign value	

Based on the depositional architecture of the Niger Delta, both the upper and lower shoreface facies are anticipated to exhibit lateral continuity across the reservoir, particularly in the east–west direction. To reflect this, an appropriate value was selected to represent their lateral extent within the model. In contrast, shorter distances were assigned for the minor direction in line with the typical dimensions and orientations of shoreface systems and associated channels in the Niger Delta basin. The distribution of facies within the three-dimensional structural and stratigraphic model was further refined by applying constraints from the Net-to-Gross (NTG) map, ensuring a geologically consistent representation.

6) Petrophysical Modelling

Evaluation and petrophysical characteristics were achieved by detailed analysis of the well log information. The outcome of this evaluation provided the source for the inputs made for the static modelling of

the reservoir. To remain compatible with the geological framework, these petrophysical characteristics were implemented within the model based on the defined facies distribution.

Critical petrophysical parameters incorporated into the model include porosity (ø), the measure of the volume of voids within the rock; gas saturation (Sg), the percentage of the volume of the pore network occupied by gas; permeability (K), the measure of the ability of the rock to pass fluid; and net-to-gross (NTG), the assessment of the volume of the reservoir-quality material within the given interval. Each of these parameters, together with the others, enables a more accurate representation of the storage and fluid-flow characteristics of the reservoir.

7) Resource Volume Calculations

Traditionally, volumetric analyses were conducted using a static model that combines the reservoir geometry with its petrophysical properties. The standard volumetric equations used are:

GIIP = GRV x N/G x Ø x Sg / Bg

STOIIP = GRV x N/G x Ø x So / Bo

Where STOIIP stands for Stock Tank Oil Initially In Place, GIIP means Gas Initially In Place.

GRV (Gross rock volume) = drainage area (acres)* reservoir thickness (feet)

NTG (net/gross ratio) = proportion of the GRV formed by the reservoir rock (range is 0 to 1)

Ø = Porosity

Gas Saturation (Sg) = the pore space of the reservoir filled with gas

Oil Saturation (So) = the pore space of the reservoir filled with oil

Gas formation volume factor (Bg) = the volume difference between the gas extracted and the gas in-situ.

Oil formation volume factor (*Bo*) = the volume difference between the gas extracted and the gas in-situ.

The *Bg* converts volumes at reservoir conditions (high pressure and high temperature) to storage and sale conditions. These parameters were derived from the static model, well logs, and core analysis. The results may be expressed as Stock Tank Oil Initially In Place (STOIIP) or Gas Initially In Place (GIIP), depending on the fluid type.

IV. RESULTS AND DISCUSSION

1) Results of Well Correlation

The correlation panels provided a graphical representation of the lateral continuity and variability of the reservoir, enabling visual tracing and interpretation of the stratigraphic and structural elements across the field. The process of flattening the correlation on these reference markers significantly improved the understanding of lateral facies variations, sedimentary geometry, and other geological characteristics such as erosional surfaces and fault intersections (Fig. 3). A notable observation from the correlation effort is the consistency in average reservoir thickness across the wells studied. This uniformity in thickness suggests a widespread and even deposition of sediments during the time of reservoir formation.

Although the reservoir showed some internal heterogeneity, the general constancy in vertical thickness implies a stable depositional regime over the area covered by the correlation. The analysis revealed a progressive increase in shaliness or heterolithic character when moving from one end of the correlation panel, designated as point A, towards the opposite end, marked as A'. This trend is interpreted as indicative of a transition in the depositional environment. The increasing shaliness suggested a shift from a more proximal, possibly fluvio-deltaic setting, toward a more distal, tidally influenced depositional regime.

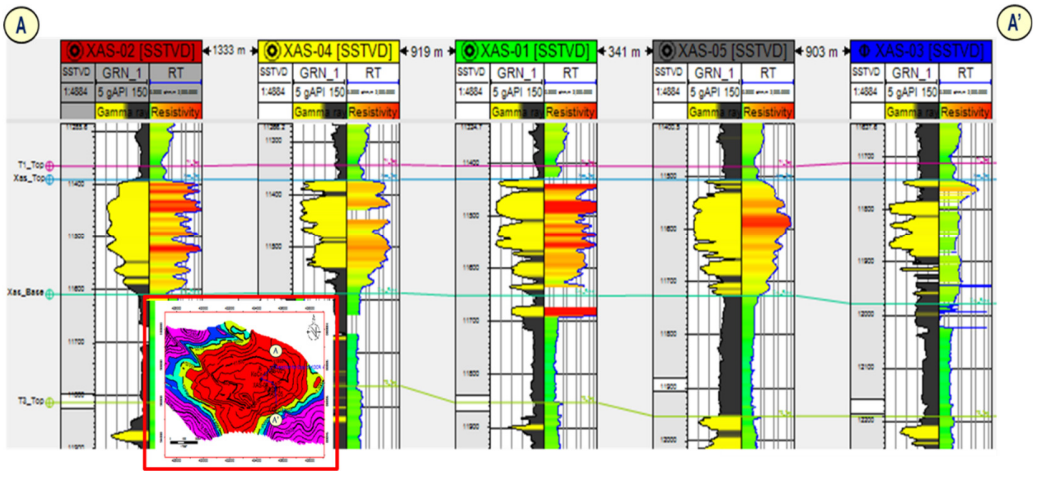

Fig. 3: Reservoir-wide dip (A-A[1]) correlation of T1 top, XAS top and base, and T3 top

The inferred environmental shift from a shallower to a deeper marine setting across the field is significant in terms of sediment characteristics. The growing tidal influence in the basinward direction is associated with an increase in heterolithic bedding, which reflects alternating deposition of sand and mud due to fluctuating energy conditions in the depositional environment.

This transition impacts key reservoir properties, particularly the net-to-gross (NTG) ratio, which represents the proportion of reservoir-quality sand relative to the total interval thickness. As the environment

becomes more heterolithic, the NTG ratio decreases accordingly, reflecting a reduced proportion of clean, sand-dominated facies.

2) Results of the Seismic Interpretation

A. Fault Interpretation

The correlation proved effective in tying the reservoir to its seismic response, providing a sound basis for further structural interpretation. Subsequent fault analysis revealed a complex fault network cutting across the reservoirs. The interpretation identified both synthetic and antithetic faults, forming a system of structural features associated with deformation processes in the area. In total, 30 individual faults were mapped from the seismic volume, signifying a highly faulted setting.

The orientation of the faults is typically east-west (E-W), and an underlying structural trend that exists in the entire study area. Two significant boundary faults, which are to the north and south of the reservoir, have been labelled as significant structural elements that can be a barrier or a trap for fluid flow in the reservoir. Fault modelling is facilitated by converting the interpreted fault sticks into fault polygons. These are used to build a structural framework of the field. The geometry and spatial relationship between faults from the observed configuration suggest that the reservoirs are positioned within the downthrown block of an E-W-trending rollover anticline. This kind of structural configuration points to the tectonic regime under which the reservoir formed. The anticlinal rollover fold indicates the likelihood that the reservoir stratigraphic units have been faulted and warped in an extensional tectonic setting. The location of the reservoir within the feature's downthrown block is confirmed by the dip and orientation of the bounding faults.

In its northern flank, control is exercised by a large-scale synthetic fault structurally, and an antithetic fault defines the south boundary. These faults not only have significant roles for the definition of the limits of the reservoir but also in understanding any potential compartmentalization in the subsurface. Figure 4 illustrates the arrangement and spatial connection between the interpreted faults and the reservoirs. These architecture statistics highlight the role of structural elements in framing the reservoir geometry and suggest the potential effect of faulting on its continuity and segmentation.

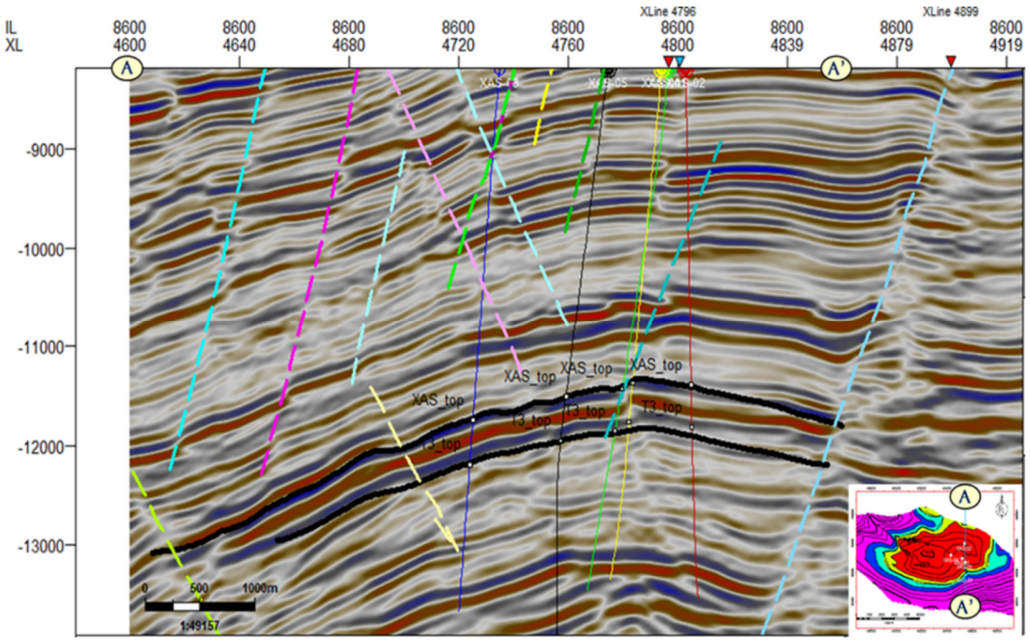

Fig. 4: In-line (8600) section showing the interpreted Faults

B. Horizon Interpretation

The interpretation of the reservoir intervals was carried out systematically, and structural grids were generated for both the XAS and T3 reservoir tops (Fig. 5). This process involved detailed seismic horizon picking and mapping to delineate the spatial distribution of the reservoirs. To enhance the accuracy of the structural interpretation, loop-tying of seismic reflectors was conducted in both the in-line and cross-line directions. This technique was particularly effective in minimizing inconsistencies, known as mis-ties, which often occur due to variations in seismic signal timing across different lines. By implementing the loop-tying method, a more coherent and geologically reasonable structural framework was achieved. The interpreted horizons were used to generate a structural grid for the reservoirs. The interpolation process smoothed the interpreted seismic data and generated a continuous time map for the reservoir units, which illustrates the configuration of the top reservoir surface.

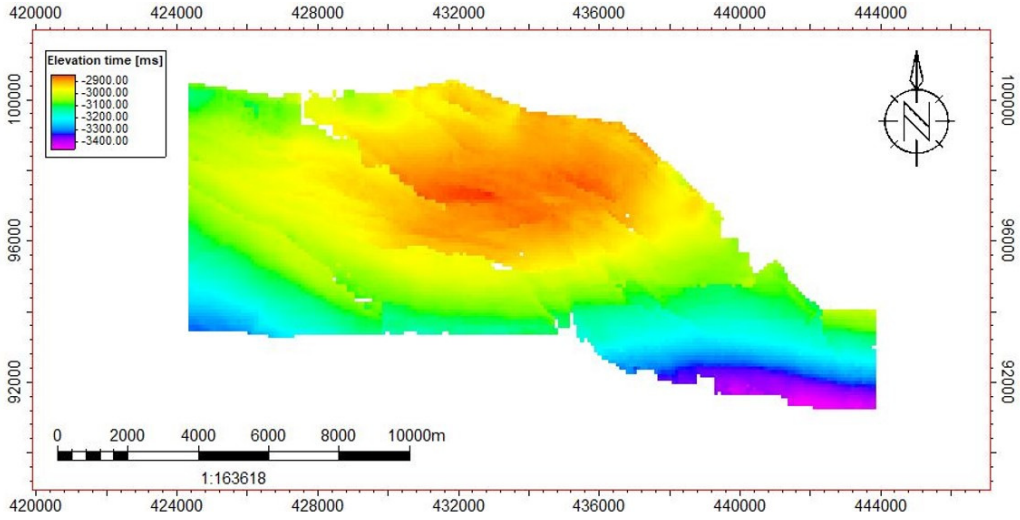

Fig. 5: Reservoir grid from horizon interpretation

C. Structural Modelling

1) Fault Modelling and Pillar Gridding

The faults identified through seismic interpretation were transformed into fault planes. Due to the simplicity of the fault geometries observed, each fault was constructed using only two shape points. This minimal configuration was adequate for accurately representing the fault surfaces, as the interpreted faults did not display significant complexity or irregularity (Fig. 6).

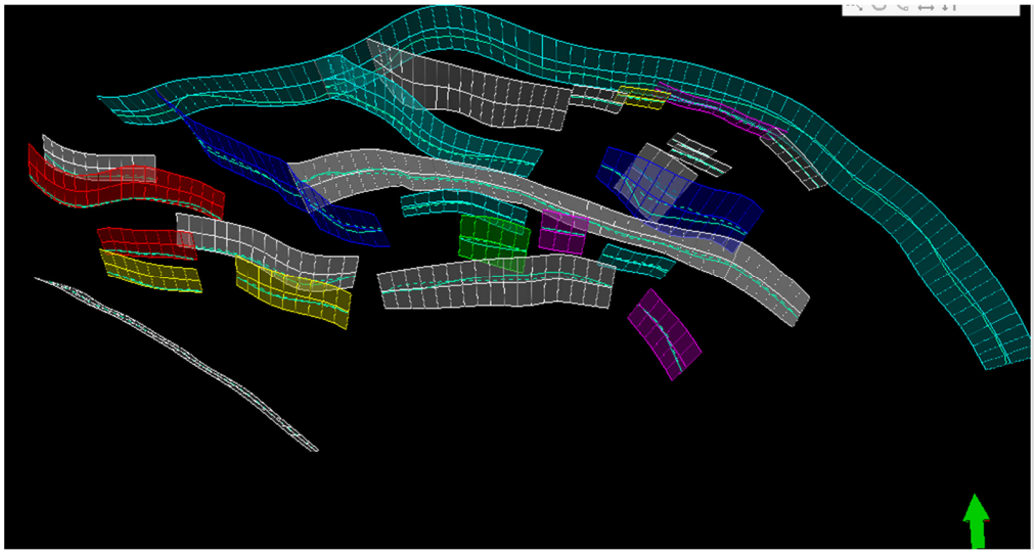

Fig. 6: 3D fault model and middle pillar grid of the XAS reservoir

During the interpretation of well data, no missing sections were observed in any of the wells that penetrated the reservoir unit. This implies a consistent geological continuity across the well paths, with no evidence of significant fault displacement that would result in the omission of stratigraphic units. Such continuity provides confidence in the accuracy of the structural framework used in the reservoir model.

To construct the three-dimensional grid framework of the reservoir, a pillar gridding method was implemented. The grid was composed of geocellular blocks, each measuring 100 meters by 100 meters along the x(i) and y(j) axes. This grid size was selected to strike a balance between computational efficiency and the level of geological detail required for accurate reservoir simulation. The relatively fine resolution of the grid ensured that important structural and stratigraphic features were captured with sufficient accuracy.

The structural modelling phase identified and incorporated a total of 26 faults within the XAS reservoir system (as illustrated in Fig. 7). A key observation from the structural model is the segmentation of the XAS reservoir into two main sections by two prominent faults, labelled F3 and F8. These faults served as major structural boundaries within the reservoir (see Fig. 8). Their orientations and displacements were significant enough to divide the reservoir into distinct compartments, each potentially behaving differently in terms of fluid flow and pressure regimes.

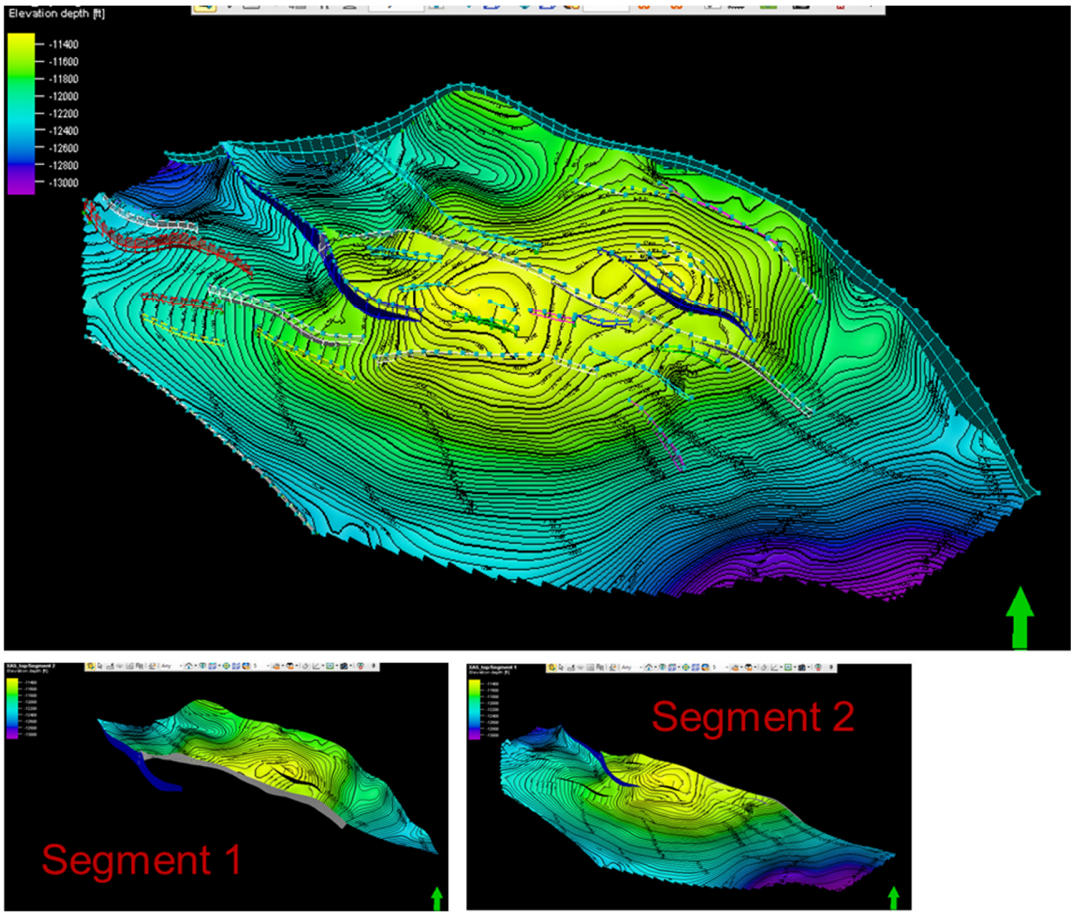

Fig. 7: Reservoir XAS and the component segments (1 and 2)

When fluid contact levels were integrated into the reservoir structure specifically, the oil-water contact (OWC) and gas-oil contact (GOC), a clearer understanding of hydrocarbon distribution emerged. By overlaying the OWC and GOC onto the structural map, it became evident that the hydrocarbon accumulations within the XAS reservoir could be categorized into two primary zones. These are referred to as the northern and southern hydrocarbon accumulations, labelled as accumulation **A** and accumulation **B**, respectively (depicted in Figs. 8 and 9).

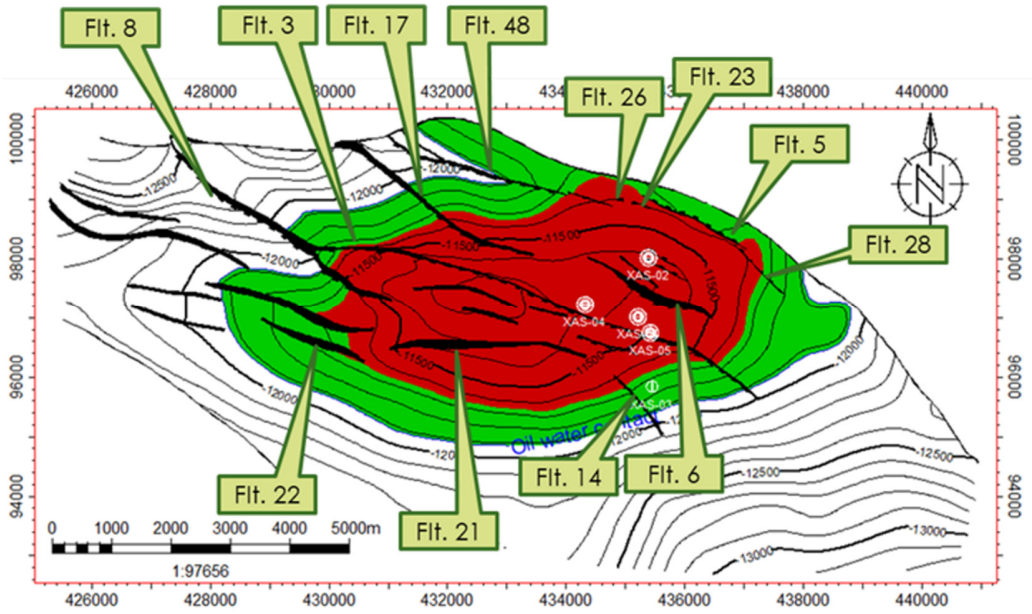

Fig. 8: Hydrocarbon distribution of the XAS reservoir and the faults cutting through the reservoir top

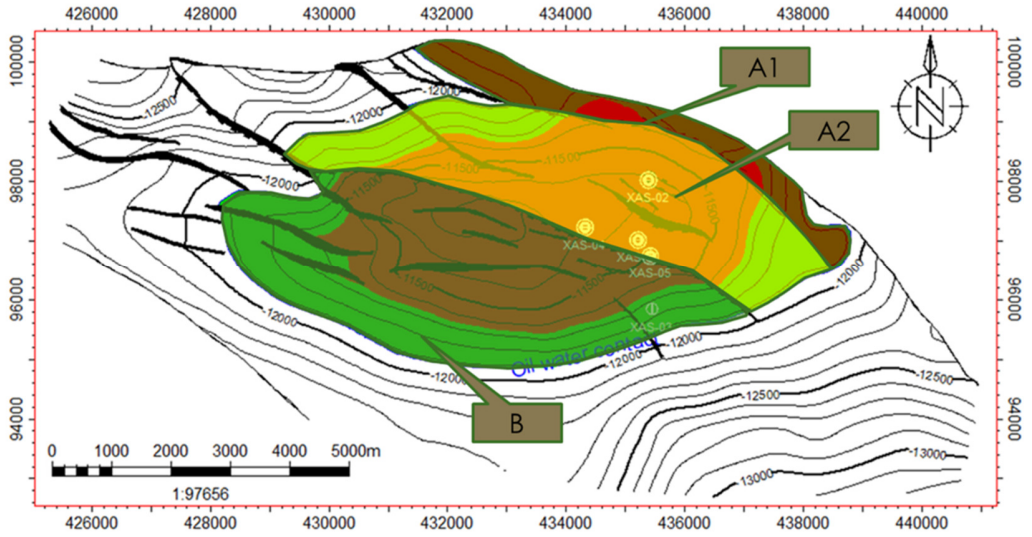

Fig. 9: Hydrocarbon distribution and likely segmentation of accumulations by the faults

Further structural analysis revealed additional compartmentalization within the northern hydrocarbon accumulation (accumulation **A**). This zone was further subdivided into two smaller structural compartments,

designated **A1** and **A2**. These sub-compartments are delineated by a series of smaller faults: F48, F23, F5, and F28. The presence of these faults suggests further internal segmentation within the northern part of the reservoir, which could have implications for both reservoir performance and development strategies.

The division of the reservoir into multiple fault-bounded compartments, first at a macro level by F3 and F8, and then at a more localized scale within the accumulation **A** by F48, F23, F5, and F28, underscores the importance of detailed structural interpretation in reservoir modelling. Such segmentation can significantly affect fluid flow, pressure support, and ultimately the recovery efficiency of the reservoir. Each compartment may respond differently to production, depending on the sealing capacity of the faults, the connectivity of the reservoir units across the fault planes, and the relative position of hydrocarbon contacts. The division of the reservoir into northern and southern accumulation zones, and further segmentation of the northern accumulation into A1 and A2 compartments, highlights the significance of fault architecture in understanding reservoir behaviour.

D. Stratigraphic Modelling and Flow Unit Correlation

Following the successful pillar gridding of the fault framework, stratigraphic modelling of the reservoir was conducted. The top of the interpreted T-reservoir served as the main bounding surface, demarcating the upper limit of the reservoir zone and helping define the vertical extent of the interval. To model the internal structure of the reservoir, the T3-reservoir base and other intermediate horizons were constructed as conformable layers, using the thickness measurements derived from well data.

The resulting structural model of the reservoir reveals that both the top and base surfaces exhibit low structural relief, with the top surface having gentle slopes along its flanks (Fig. 10). Structurally, the XAS reservoir is characterized as a rollover anticline with a northwest–southeast orientation. This structural style indicates that the reservoir formed in response to extensional deformation, specifically related to movement along major growth faults along the northern boundary. As the underlying sediments were displaced, differential loading and fault movement caused the overlying strata to bend and form the observed rollover geometry. Crestal faulting seen in the model likely developed as a consequence of continued deformation during this rollover process, contributing to the present-day complexity of the structural trap.

The interpretation of flow units within the reservoir was aided by a combination of electrofacies analysis and the integration of well log data, particularly gamma ray (GR) logs. The electrofacies data, interpreted from wireline log responses, made it possible to distinguish five primary lithofacies within the reservoir: channel sandstones, upper shoreface sands, lower shoreface sands, heterolithic units, and shale layers. These facies are key in defining both the depositional environment and reservoir quality.

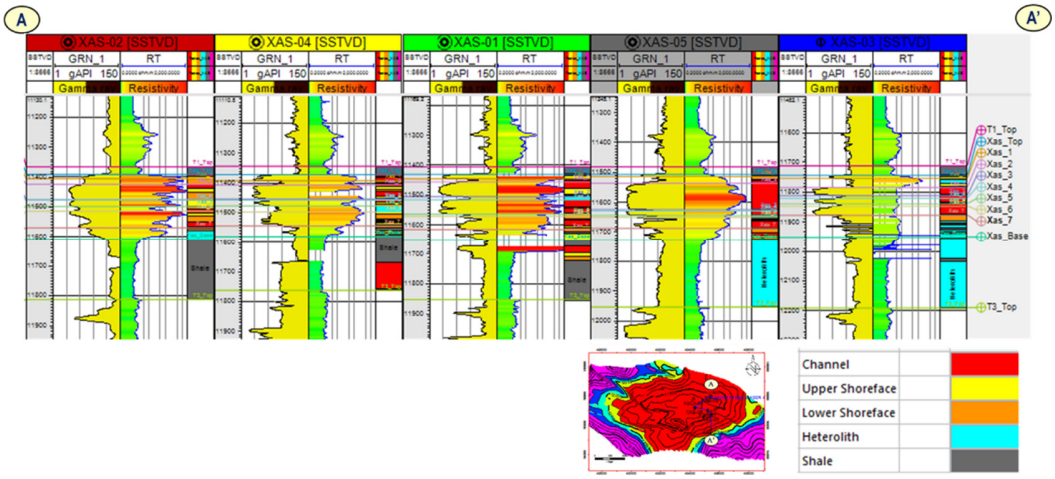

Figure 10: The internal correlation and facies description of the XAS field and reservoir zonation

Based on these interpretations, two primary flow units were delineated within the reservoir. These flow units represent zones of enhanced reservoir connectivity and permeability, driven by the dominance of higher-quality sand-rich facies. In general, the reservoir exhibits a vertical trend of decreasing quality with depth. Near the top of the reservoir, cleaner and coarser-grained facies such as upper shoreface sands and channel sandstones are predominant. These facies are typically well-sorted and possess good porosity and permeability characteristics, making them favourable for hydrocarbon flow. However, moving downward within the reservoir interval, the facies become increasingly fine-grained and heterolithic, with a higher presence of shales, leading to a reduction in reservoir quality.

Seven distinct zones were identified within the XAS reservoirs based on stratigraphic and facies characteristics. Each of these zones represents a different stage or style of deposition and has unique reservoir properties. The stratigraphic modelling undertaken after fault gridding provided a coherent framework for understanding the internal geometry and depositional evolution of the XAS reservoirs.

E. Geological Modelling Using Facies and Petrophysical Logs

To construct reliable geological models of the reservoir, the available facies and petrophysical well log data were subjected to an upscaling process. The parameters used for the upscaling of well logs are presented in Table 4.1, providing the basis for consistent modelling across the entire study area.

Table 2: Log upscaling parameters

Logs	Use Bias	Average Method	Treat Log as:	Method
Facies	No	Most of	Lines	Neighbour cell
Porosity	Facies	Arithmetic	Points	Neighbour cell
Net to Gross	Facies	Arithmetic	Points	Neighbour cell

To quantify and assess the uncertainties inherent in hydrocarbon volume estimations, multiple realizations of the geological models were generated. Specifically, three separate realizations of both facies and petrophysical models were developed for each of the three modelling algorithms employed. An essential part of this modelling process involved constraining the petrophysical models to the facies models. This technique is widely recognized for improving the geological realism of reservoir properties such as porosity and permeability.

By linking petrophysical properties directly to the geological environment in which they were deposited, the models become more geologically consistent and better represent the reservoir's internal architecture. Visual interpretations of the modelled facies are shown in Figure 11. These results exhibit a high degree of correlation with previously interpreted well data and geological facies descriptions. The model successfully replicates the spatial arrangement of sedimentary structures observed in the field. Notably, the dominant depositional environments identified in the model include channelized and shoreface systems. These environments are characterized by their distinct sediment transport and deposition processes, which directly influence reservoir quality.

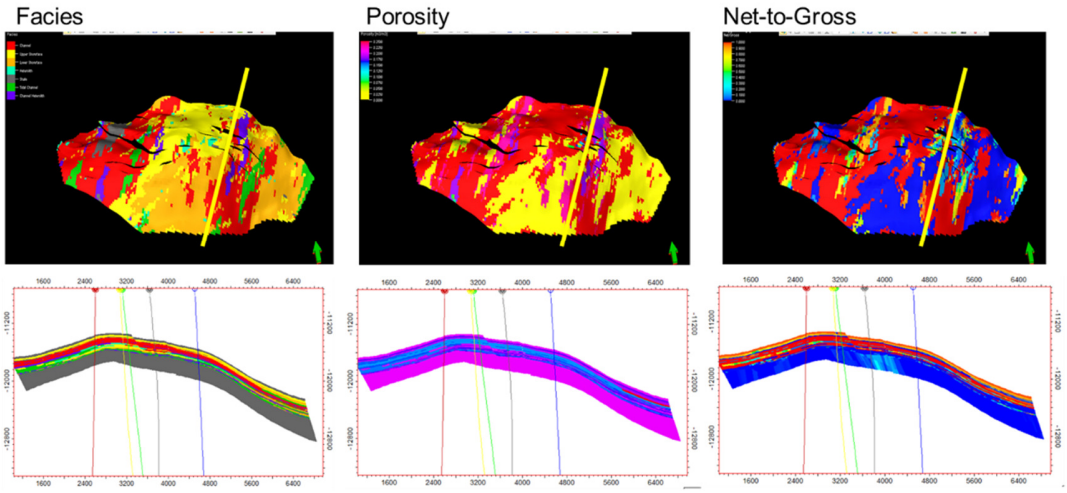

Fig. 11: Modelled facies and petrophysical properties and their cross sections

The shoreface facies are observed to extend predominantly in the east-west direction. This extensive lateral continuity suggests a high-energy shoreline system that prograded over time, possibly in response to relative sea-level changes. In contrast, the channel facies are more localized and tend to follow a north-south orientation. These channels are interpreted as incised features that cut through the existing shoreface deposits, indicating multiple phases of sediment input and possible fluvial influence. Petrophysical property analysis of the XAS reservoir reveals a distinct variation in porosity and permeability across different stratigraphic zones. The porosity values show a downward trend from shallower to deeper zones.

Table 3: Average petrophysical properties for the XAS reservoir

Zone Names	Average NTG	Average Porosity	Average Permeability (mD)	Average SW
Xas_1	0.35	0.29	307.16	0.064
Xas_2	0.32	0.33	1028.37	0.023
Xas_3	0.68	0.27	398.67	0.040
Xas_4	0.41	0.34	2430.55	0.038
Xas_5	0.72	0.30	452.06	0.068
Xas_6	0.43	0.30	336.77	0.043
Xas_7	0.28	0.17	312.10	0.237

The integration of well data, facies interpretation, petrophysical analysis, and geostatistical modelling exemplifies a multidisciplinary approach to reservoir characterization. Each component contributes to building a coherent and realistic representation of the subsurface. Upscaling ensures compatibility with reservoir simulation grids, facies modelling delineates depositional environments, and petrophysical modelling quantifies the reservoir's capacity to store and transmit fluids.

The geological modelling workflow carried out in this study demonstrates the effectiveness of integrating facies and petrophysical data to construct high-resolution, geologically consistent models. The results highlight the predominance of channel and shoreface facies, with significant variations in porosity and permeability across stratigraphic zones.

By using multiple realizations and algorithmic approaches, the study accounts for geological uncertainty and enhances the reliability of hydrocarbon volume estimates. The constrained petrophysical models, which align closely with facies distributions, underscore the importance of geological context in reservoir property modelling.

F. Fault Seal Analysis

1) Fault Zone Juxtaposition

A comprehensive fault juxtaposition analysis was carried out on all the intra-reservoir faults that intersect the XAS reservoir (Figure 12 B). This analysis was aimed at understanding the potential for fault-related compartmentalization and seal behaviour within the reservoir. Figure 12 presents the juxtaposition relationships across all the identified faults within the XAS reservoir. The boundary faults do not exhibit any juxtaposition, which is attributed to the modelling approach, where the XAS reservoir was constructed independently from the surrounding reservoirs in the field. This isolation in the model prevents any fault block interaction across reservoir boundaries, which in turn affects the interpretation of fault sealing capacity at the field scale. The absence of juxtaposition in the boundary faults reinforces the compartmentalized nature of the reservoir model.

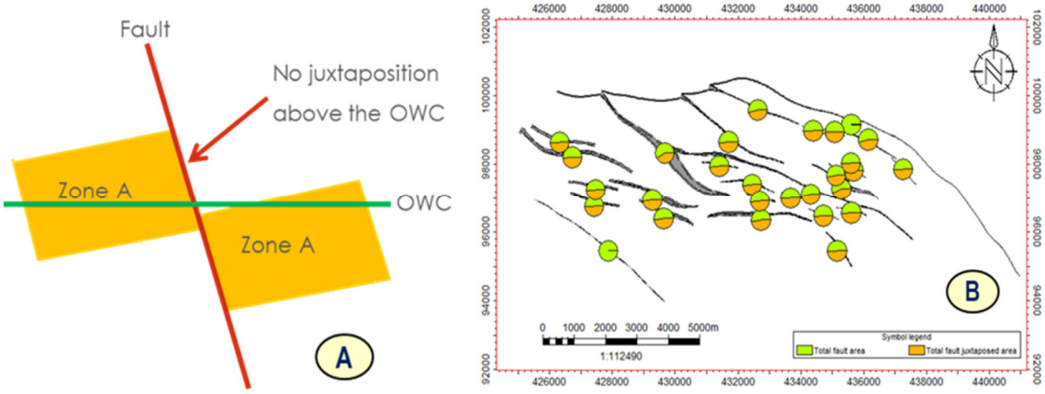

Fig. 12 (A &B): (**A**) Allen diagram showing juxtapositions, (**B**) 2D view of the faults and their juxtaposition amounts

Furthermore, Figure 13 highlights the zones of effective juxtaposition that are situated above the oil-water contact (OWC). These upper sections are particularly important for evaluating the sealing behaviour of faults, as they directly influence the trapping potential of hydrocarbons.

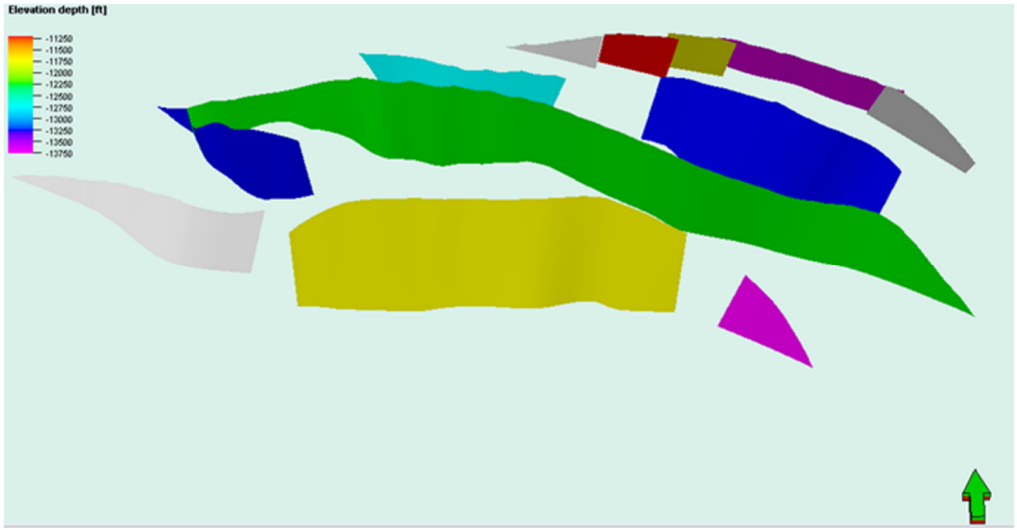

Fig. 13: 3D view of the faults and their reservoir on the reservoir (sand-on-sand) juxtaposed fault faces

2) Fault Zone Thickness

The thickness of fault zones in the juxtaposed areas of both faults varies between approximately 2.5 feet and 5 feet. This measured range is significant in understanding the potential behaviour of fluids within the reservoir. Faults with such thickness are generally considered permeable enough to allow crossflow of hydrocarbons between adjacent compartments or reservoir blocks. This crossflow can have considerable implications for reservoir management, production strategies, and overall recovery efficiency. When faults are thin, they may act as barriers; however, in this case, the observed thickness range suggests that the faults are not completely sealing. Instead, they may permit the movement of hydrocarbons across them, impacting pressure

communication and fluid distribution in the field. Figure 14 provides a visual representation of this phenomenon, illustrating how the fault thickness contributes to the possibility of hydrocarbon migration.

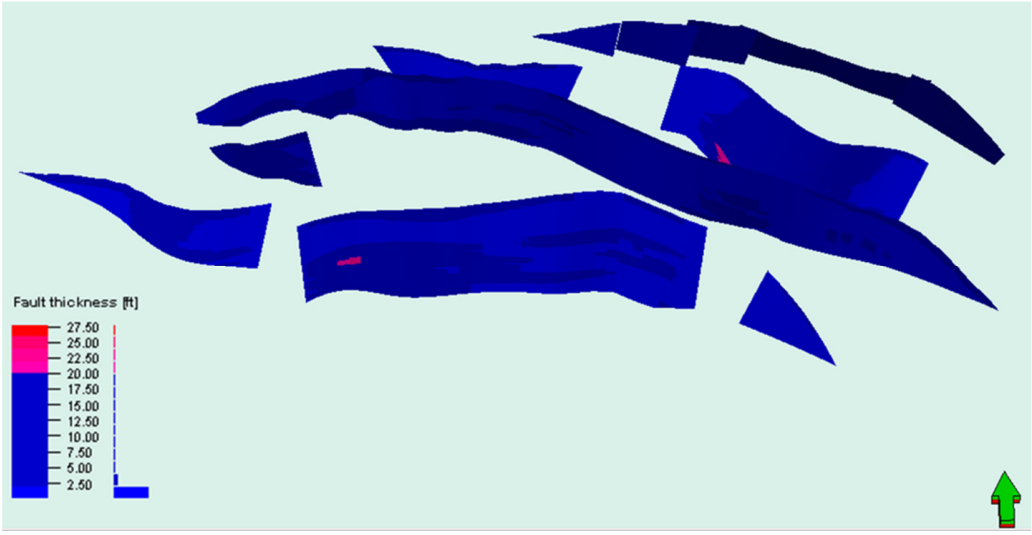

Fig. 14: fault zone thickness of the XAS faults

3) Fault Zone Permeability

Fault zone permeability was evaluated by integrating the permeability of the undeformed reservoir rock with the Shale Gouge Ratio (SGR) values calculated along the fault zones. This method provides an estimate of how much deformation and clay content may influence fluid flow across faults. The resulting fault permeability values for the juxtaposed sections of the analyzed faults range from approximately 500 millidarcies (mD) to 10,500 mD, as illustrated in Figure 15. These relatively high permeability values indicate that the faults are likely to be transmissive, facilitating potential crossflow of fluids between adjacent reservoir compartments. Such behaviour implies a reduced sealing capacity in these specific fault segments, which is a critical consideration in reservoir modelling and hydrocarbon recovery planning. The results align with previous studies, such as those by Yielding *et al.* (2010), which also noted the potential for crossflow in fault zones exhibiting similar permeability characteristics and low sealing potential.

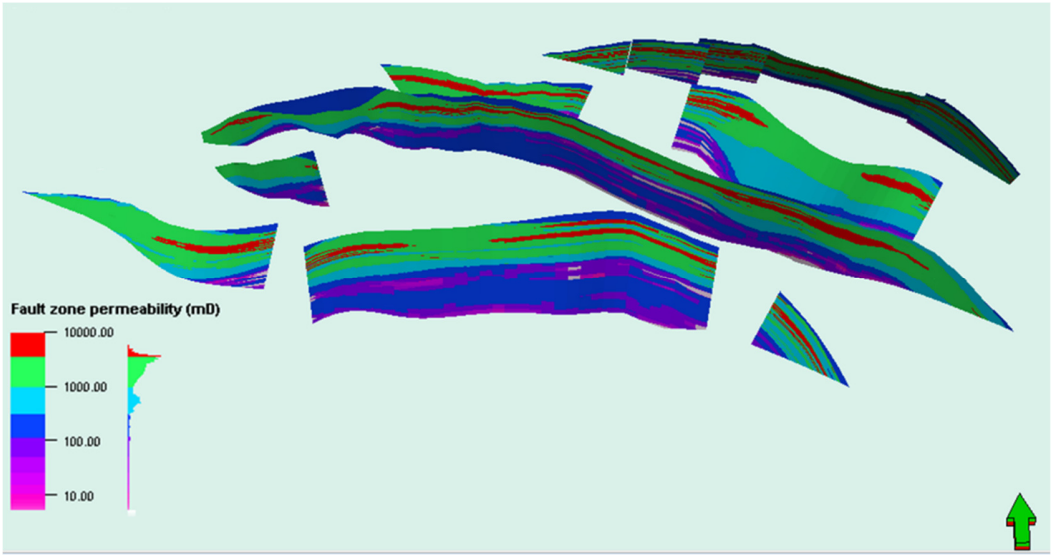

Fig. 15: Fault zone permeability of the XAS faults

4) Fault Zone SGR

The Shale Gouge Ratio (SGR) in the study area ranges from approximately 10% to 25%. These values are all below the commonly accepted threshold of 30%, which is considered the limit above which faults typically act as seals to fluid flow. Since all observed SGR values fall under this threshold, it suggests that the majority of the faults present are likely to permit cross-fault flow. This indicates a higher potential for hydrocarbon migration across these faults, enhancing the connectivity of reservoir units. Therefore, the faults with SGR below 30% are expected to be non-sealing and would allow hydrocarbons to pass through, potentially aiding reservoir communication and production.

However, a few localized zones exhibit SGR values above 30%, and these areas have been highlighted with black circles in Figure 16. Faults within these zones are likely to restrict fluid movement due to increased shale content in the fault gouge material, which could result in sealing behaviour. These high-SGR zones may serve as baffles or partial barriers that could compartmentalize the reservoir and influence fluid distribution. Recognizing and mapping these variations in SGR is essential for assessing fault seal integrity, predicting hydrocarbon entrapment, and designing effective reservoir management strategies.

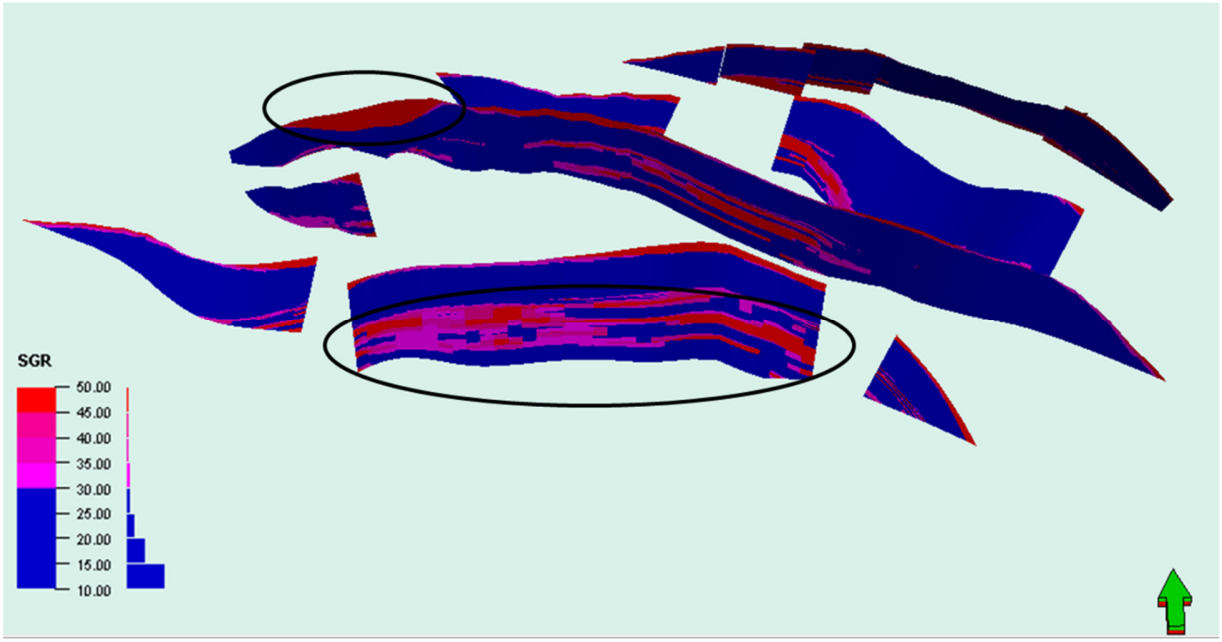

Fig. 16: Fault zone SGR, showing part of the area above the 30% SGR that will not permit fluid crossflow

G. Volume Calculations

Hydrocarbon volume assessments for the XAS reservoir have yielded a Stock Tank Oil Initially In Place (STOIIP) of 805 million STB and a Gas Initially In Place (GIIP) of 1312 million MSCF. These volume estimates are detailed in Table 3. The analysis reveals that the largest quantities of both oil and gas are located in Area **B**. This area stands out as the most promising zone for hydrocarbon extraction within the reservoir. On the other hand, Area **A1**, which does not have any well penetration, has not been directly evaluated for hydrocarbon volumes. While there is no direct well data, the fault that separates Area **A1** from Area **A2** is not considered to be a significant compartmentalizing factor.

It is assumed that this fault does not create isolated sections that would hinder hydrocarbon accumulation in Area **A1**. However, it is important to note that this fault could potentially act as a barrier to the lateral flow of hydrocarbons, possibly acting as a baffle. This could limit the movement of fluids across the fault line and affect the distribution of oil and gas between the two areas. Despite this, it is believed that the overall reservoir integrity remains intact and that Area **A1** may still hold recoverable volumes, albeit with some constraints on flow dynamics due to the fault's presence.

Table 4: Volumetrics for the different regions of the XAS reservoir

	STOIIP [*10^6 STB]	**GIIP [*10^6 MMSCF]**
Total Vol.	805	1312
Vol. (A1)	147	161
Vol. (A2)	185	360
Vol. (B)	473	791

V. CONCLUSION

In conclusion, the integration of seismic data, fault analysis, facies distribution, and volumetric calculations provided a comprehensive and multifaceted understanding of the XAS reservoir's characteristics. Seismic data offered a clear view of the subsurface structures, allowing for the identification of fault lines and potential fluid pathways, while fault analysis helped to assess the impact of fault compartments on fluid movement and reservoir performance. By evaluating facies distribution, insight into the heterogeneity of the reservoir, which is crucial for understanding variations in permeability and porosity, was gained. Additionally, the volumetric calculations provided essential estimates of the hydrocarbon volumes present, which are vital for determining the reservoir's commercial viability.

Furthermore, the combination of geological modelling with a detailed understanding of fault behaviour and fluid dynamics enhances the ability to forecast reservoir performance over time. This knowledge allows for the development of more effective production strategies that take into account both immediate and long-term recovery goals. Ultimately, this holistic approach ensures that the full potential of the XAS reservoir is realized, leading to increased profitability and more sustainable reservoir management.

ACKNOWLEDGEMENTS

The authors wish to thank the reviewers of the manuscript and the management of the Shell Petroleum Development Company Nigeria (SPDC), now Renaissance Africa Energy Company (RAEC), for providing the data for the research, without which this study would not have been a success.

REFERENCES

[1] Adekunle, A., and Aizebeokhai, A. P. (2020). Fault-Bounded Compartmentalization in Turbiditic Reservoirs of the Niger Delta. *Journal of Petroleum Science and Engineering*, 187, 106757.

[2] Aderoju, S., Igho, F.A., & Asuquo, O.E (2019). Fault Seal Integrity in the Niger Delta. *Petroleum Geoscience*, 25(4), 467-482.

[3] Berg, R.R. (1975). Capillary pressure in stratigraphic traps: *American Association of Petroleum Geologists Bulletin*, 59, 939–956.

[4] Bretan, P., Yielding, G., & Freeman, B. (2003). An empirically based method for predicting fault seal capability. *American Association of Petroleum Geologists Bulletin*, 87(6), 807–821.

[5] Bretan P., Yielding G., and Jones H. (2003). Using calibrated shale gouge ratio to estimate hydrocarbon column heights: *American Association of Petroleum Geologists Bulletin*, 87, 397–413.

[6] Corredor, F., Shaw, J.H., and Bilotti, F. (2005). Structural styles in the deep-water fold and thrust belts of the Niger Delta. *American Association of Petroleum Geologists Bulletin*, 89, 753 - 780.

[7] Doust, H., & Omatsola, E. (1990). Niger Delta. In J. D. Edwards & P. A. Santogrossi (Eds.), Divergent/passive margin basins (Vol. 48, pp. 239–248). *American Association of Petroleum Geologists* Memoir

[8] Fisher, Q. J., & Knipe, R. J. (2001). The permeability of faults within siliciclastic petroleum reservoirs of the North Sea and Norwegian Continental Shelf. *Marine and Petroleum Geology*, 18(10), 1063–1081.

[9] Freeman, P., Freeman, S.R., Harris, S.D. & Knipe, R.J. (2010). Fault Compartmentalization in the North Sea. *Geological Society of London Special Publications*, 344, 271-286.

[10] Jolley, S.J., Barr, D., Walsh, J.J. and Knipe, R.J. (2007a). Structurally Complex Reservoirs: *An Introduction*. *Geological Society*, London, Special Publications, 292.

[11] Jolley, S.J., Dijk, H., Lamens, J.H., Fisher, Q.J., Manzocchi, T., Eikmans, H., and Huang, Y. (2007b). Faulting and fault sealing in production simulation models: Challenges and Impact of Compartmentalization, Brent province, northern North Sea: *Petroleum Geoscience*, 13, 321–340.

[12] Knipe, R. J. (1997). Juxtaposition and seal diagrams to help analyze fault seals in hydrocarbon reservoirs. *American Association of Petroleum Geologists Bulletin*, 81(2), 187-195.

[13] Lehner, P., & De Ruiter, P. A. C. (1977). Structural history of the Atlantic margin of Africa. *American Association of Petroleum Geologists Bulletin*, 61(7), 961–981.

[14] Lindsay, N.G., Murphy, F.C., Walsh, J.J. and Watterson, J. (1993). Outcrop studies of shale smear on fault surfaces: *International Association of Sedimentologists* Special Publication 15, 113–123

[15] Lindsay, R., *et al.* (1993). The Effect of Clay Smear on Fault Sealing. *American Association of Petroleum Geologists Bulletin*, 77(6), 1153-1162.

[16] Obaje, N.G., Akinola, J.A. Afolabi, M.O. & Oguike, A.A. (2021). Stress Perturbations and Seal Failure in Faulted Zones. *Geotechnical Research*, 21(5), 123-136.

[17] Watts, N.L. (1987). Theoretical aspects of cap-rock and fault seals for single- and two-phase hydrocarbon columns: *Marine and Petroleum Geology*, 4, 274–307.

[18] Yielding, G., Gaskill, J.G. & Smith, A.E. (1997). Fault Seals and Sealing Mechanisms in Hydrocarbon Reservoirs. *Journal of Petroleum Geology*, 20(4), 365-389.

[19] Yielding, G., Freeman, B., & Needham, D. T. (1997). Quantitative fault seal prediction. *American Association of Petroleum Geologists Bulletin*, 81(6), 897–917.

